Asian Journal of Chemistry; Vol. 24, No. 4 (2012), 1798-1804

ASIAN JOURNAL OF CHEMISTRY

www.asianjournalofchemistry.co.in

Theoretical Studies of the Reaction Paths and Rate Constants for SiH_4 + H System

CHUANSONG QI[1] and XIAOMIN SUN[2,3*]

[1]College of Chemical Engineering, Beijing Institute of Petrochemical Technology, Beijing 102617, P.R. China
[2]State Key Laboratiory of Solid Lubrication, Lanzhou Institute of Chemical Physics, Chinese Academy of Science, Lanhou 730000, P.R. China
[3]Environment Research Institute, Shandong University, Jinan 250100, P.R. China

*Corresponding author: Fax: +86 531 88364416; E-mail: sxmwch@sdu.edu.cn

(*Received*: 3 May 2011; *Accepted*: 28 November 2011) AJC-10765

The reaction of SiH_4 with H has been studied using the three *ab initio* levels. The structure of the potential energy surface includes the reactants, the prior complex, the transition state, the post-complex and the product, are reported. Along the reaction coordinates, the dynamic potential wells correspond to the Feshbach resonance. The rate constants are calculated using the TST (CVT, ICVT) methods with the SCT correction. Rate constants in the temperature range of 200-1600 K were reported at the G2//QCISD/6-311+G(df,pd) level and exhibits typical non-Arrhenius behaviour. The viriational effect on the values of rate constant is small and the tunneling correction is important in the calculation of rate constants in the lower temperature range. The three parameters expression in the range 200-1600 K is $cm^3\ mol^{-1}$. The calculated ICVT/SCT rate constants are in good agreement with the available experimental data.

Key Words: Direct dynamics studies, Variational transition-state theory, H + SiH_4 System, *Ab initio* potential energy surface, Rate constants.

INTRODUCTION

The reaction of H with SiH_4 has been concerned in the last three decades by both theoretician and experimentalist because it plays a significant part in the chemical vapour deposition (CVD) processes used in the semiconductor industry[1-5]. In experiments, Arthur *et al.*[6] had investigated the temperature dependence of the rate constants, *i.e.* $k = (2.3 \pm 0.3) \times 10^{-11} \exp[(-11.6 \pm 0.3\ kJ/mol)/RT]\ cm^3\ s^{-1}$, in the temperature range 294-487 K. Goumri *et al.*[7], reported the rate constants in the temperature range 290-660 K to be $k = (1.78 \pm 0.11) \times 10^{-10} \exp[(-(16.0 \pm 0.2)\ kJ/mol)/RT]\ cm^3\ s^{-1}$. As for other experimental results, they concerned the rate constants[8-12] or the pressure dependence of the rate constants[13] at an isolated temperature, mainly at or near the room temperature. On the other hand, many theoretical investigations have been reported on the rate constants including the semiempirical method and the first principle. Michael *et al.*[9] and Gaspar *et al.*[10] calculated the activation energies using the bond-energy-bond-order (BEBO) methods in 1974 and in 1975, respectively. Gordon *et al.*[14] and Tachibana *et al.*[15] studied the stationary points on the reaction path based on Hartree-Fock level of theory excluding correlation correction, therefore they did not obtain satisfactory reaction barrier and reaction enthalpy. Goumri *et al.*[7] made a further study on the reaction rate constants using the non-variational transition state theory with Wigner tunneling correction. Basing on MP2/6-31G* optimized geometries and the G2 energy correction, the reaction enthalpy is in agreement with the experimental value. However, due to the limits of method, the calculated imaginary frequency of transition state (TS) is too large, which will narrow the potential barrier and over estimate the tunneling correction. Dobbs *et al.*[16] predicted the activation energies for the abstraction and exchange reactions of H with SiH_4 at the QCISD(T)//MP2/TZ+2p+f level and given the rate constants using transition-state-theory with Wigner tunneling correction. Espinosa *et al.*[17], calculated of rate constants and kinetic isotope effects with variational transition-state theory (VTST) over the temperature range 200-1000 K through constructing a semiempirical analytical potential energy surface (PES). Yu *et al.*[18] performed the direct dynamics studies using *ab initio* molecular orbital theory (at the level G2//UQCISD/6-311+G**) and the canonical variational transition state theory with small curvature tunneling correction. The rate constants can be expressed as $k = 2.27 \times 10^5\ T^{2.69} \exp(-779/T)\ cm^3\ mol^{-1}\ s^{-1}$. It should be pointed out that the theoretical levels used in calculation are low or the potential energy surface adopted in the dynamic calculation is semiempirical in the above theoretical studies. And the dynamic properties are still not in agreement well with the experimental results. So higher level theory should be adopted and high accuracy *ab initio* potential energy surface should be reconstructed. Recently, Wang *et al.*[19] constructed a global

12-dimensional *ab intio* potential energy surface at the UQCISD/CC-PVTZ level. The title system still is necessary to make a further study including the construction of the potential energy surface with high accuracy, the calculation of the reactive probability, cross section and rate constants.

The objective in embarking on the present work is to make a further systematic theoretical investigation of the SiH_4 + H system. The direct dynamic methods are applied to calculate the reaction rate constants over a wide temperature range. An improved Shepard interpolation method will be used to construct the global PES in next step. The electronic structure information obtained from *ab initio* method is enough to calculate the rate constants using the direct dynamic method. According to the result of direct dynamics, a suitable theoretical method and basis set can be chosen to prepare the electronic structure information. On the basis of enough data points, the global PES can be obtained using an improved Shepard interpolation method.

COMPUTATIONAL METHOD

Direct dynamic methods use electronic structure information, including geometries, energies, gradients and force constants at selected points on the reaction path to calculate rate constants. Usually the direct dynamic calculation is carried out in two stages:

In the first stage, *ab initio* calculations are performed for stationary points and for some extra points along the minimum energy paths (MEP) to obtain potential energy information. Here the optimized geometries and frequencies of the stationary points (reactants, transition states and products) are calculated at three levels, *i.e.*, UQCISD/6-311+G**, UQCISD/6-311++G(df,pd), UQCISD/CC-PVTZ. From those levels, UQCISD/6-311++G(df,pd) is chosen to prepare the electronic structure information. The minimum energy paths are calculated with a gradient step size of 0.05 (amu)1/2 bohr in mass-weighed Cartesian coordinates and the harmonic vibrational frequencies as well as the force-constant matrixes at the selected points along the minimum energy paths are obtained. The shape of the minimum energy paths is important for the calculation of rate constants. The energies of the minimum energy paths are refined by the G2//UQCISD method, which implies that G2 method[20] should be used to calculate the energies according to the stationary point geometries and the selected points along the minimum energy paths obtained at the UQCISD/6-311++G(df,pd) level. The *ab initio* work is performed in Gaussian 03 program[21].

In the second stage, the potential energy information is used to calculate the rate constants and its temperature dependence with variational transition state theory which is based on the idea of varying the dividing surface along a reference path to minimize the rate constant. In this paper, the rate constants are calculated using the canonical variational transition state theory (CVT) and the improved canonical variational transition state theory (ICVT) with zero-curvature tunneling correction (ZCT) and small-curvature tunneling correction (SCT). The direct dynamic work is performed in POLYRATE 9.3.1 program[22].

RESULTS AND DISCUSSION

The optimized geometries and frequencies of the reactant, intermediates, transition states and products can be found in Tables 1 and 2, respectively. Tables 3 and 4 listed the energies, reaction enthalpies and potential barriers of stationary points at different levels, respectively. Rate constants for the reaction $SiH_4 + H \rightarrow SiH_3 + H_2$ in the temperature range 200-1600 K at the G2//QCISD/6-311++G(df,pd) level are listed in Table-5. The atomic numbers are labeled in **Scheme-I**. The profile of the reaction path is drawn in Fig. 1. The main geometry parameters varying with the reaction coordinate are listed in Fig. 2. Fig. 3 shows the classical potential energy, vibrationally adiabatic potential energy and the ZPE curves as functions of s. The changes of the generalized normal-mode vibrational frequencies as functions of s are drawn in Fig. 4. Fig. 5 shows the potential energy curves of the V_{MEP} plus the vibrational energy ε_n (n = 0, 1, 2, 3, 4) along the reaction path. Finally, the forward rate constants including theoretical and experimental results are shown in Fig. 6.

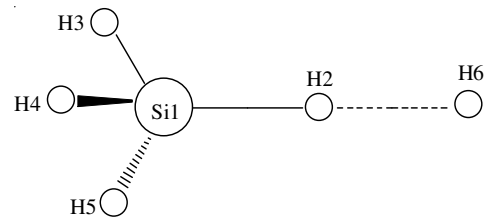

Scheme-I: Atomic numbers for the reaction $SiH_4 + H \rightarrow SiH_3 + H_2$

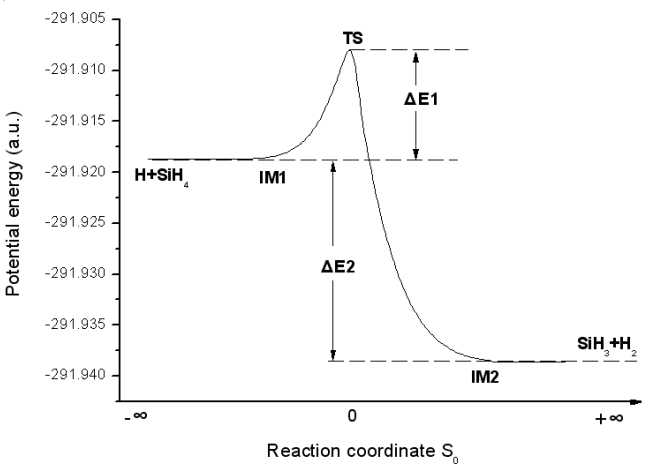

Fig. 1. Profile of the reaction path of the reaction $SiH_4 + H \rightarrow SiH_3 + H_2$ at the QCISD/6-311++G(df,pd) level

Information of stationary points: Apart from the theoretical results of the geometry parameters, some available experimental results are also listed in Table-1. It can be seen that the optimized parameters of the reactants and products are in good agreement with the experimental data at three *ab initio* levels. Concretely, the parameters obtained at the QCISD/CC-PVTZ level is best, those obtained at the QCISD/6-311++G(df,pd) level take second place and those obtained at the QCISD/6-311+G** are in the third place. The change of frequencies in Table-2 has the same trend. It can be expected that the calculation has the reliable accuracy. At the QCISD/

TABLE-1
GEOMETRICAL PARAMETERS OF STATIONARY POINTS AT DIFFERENT LEVELS
(DISTANCES IN ANGSTROMS AND ANGLES IN DEGREES)

Stationary points	Geometrical parameters	*Ab initio* method			Experiment value
		QCISD/6-311+G**	QCISD/6-311++G(df,pd)	QCISD/CC-PVTZ	
SiH_4 (Td)	r_{SiH}	1.4766	1.4772	1.4820	1.4798
SiH_3 -H'-H''(C_{3v}) (IM1)	$r_{H'-H''}$	3.6390	3.6390	3.6380	
	$r_{SiH'}$	1.4770	1.4770	1.4770	
	r_{SiH}	1.4771	1.4771	1.4771	
	<H'H''Si	180.0	180.	180.	
	<HSiH'	109.4712	109.4714	109.4700	
SiH_3 –H'-H''(C_{3v}) (TS)	$r_{H'-H''}$	1.1275	1.1301	1.1507	
	$r_{SiH'}$	1.6008	1.5991	1.5983	
	r_{SiH}	1.4770	1.4774	1.4818	
	<H'H''Si	180.000	180.0000	180.0000	
	<HSiH'	108.6207	108.5989	108.6516	
SiH_3 –H'-H''(C_{3v}) (IM2)	$r_{H'-H''}$	0.7436	0.7431	0.7431	
	$r_{SiH'}$	4.1621	4.1613	4.1615	
	r_{SiH}	1.4772	1.4765	1.4770	
	<H'H''Si	180.0	180.	180.	
	<HSiH'	111.2375	107.1624	108.15304	
SiH_3 (C_{3v})	r_{SiH}	1.4777	1.4764	1.4827	
	<HSiH	111.2471	111.6942	111.2002	
H_2	$r_{H'H''}$	0.7436	0.7430	0.7429	0.7414

TABLE-2
VIBRATIONAL FREQUENCIES (cm^{-1}) OF STATIONARY POINTS AT DIFFERENT LEVELS AND EXPERIMENTAL RESULTS

Stationary points	*Ab initio* method			Experiment value
	QCISD/6-311 +G**	QCISD/6-311++G(df,pd)	QCISD/CC-PVTZ	
SiH_4 (Td)	(T2)960, (E)996, (A1)2299, (T2)2303	(T2)956, (E)975, (A1)2299, (T2)2303	(T2)939, (E)989, (A1)2257, (T2)2263	(T2)914, (E)975, (A1)2187, (T2)2191
SiH_3 –H'-H''(C_{3v})(TS)	(E)312,(A1)907, (E)969,(E)1006, (A1)1150, (A1)2286, (E)2302, (A1)1398i	(E)276, (A1)905, (E)924,(E)967, (A1)1159, (A1)2289, (E)2303, (A1)1355i	(E)284(A1)891, (E)951, (E)987, (A1)1153, (A1)2249, (E)2266, (A1)1332i	
SiH_3 (C_{3v})	(A1)806, (E)902, (A1)2266, (E)2298	(A1)797, (E)958, (A1)2275, (E)2307	(A1)784, (E)946, (A1)2227, (E)2261	
H_2	(Σ_g^+) 4419	(Σ_g^+)4437	(Σ_g^+)4406	(Σ_g^+) 4403

TABLE-3
ENERGIES (a.u.) OF STATIONARY POINTS AT DIFFERENT LEVELS

	Q^a	$G2//Q^a$	$MRCI^a//Q^a$	Q^b	Q^b + ZPE	$G2//Q^b$	$MRCI^b//Q^b$	Q^c	Q^c + ZPE
H	-0.49981	-0.50000	-0.49982	-0.49982	-0.49982	-0.49764	-0.49982	-0.499810	-0.499810
SiH_4	-291.36902	-291.41847	-291.44428	-291.41888	-291.38692	-291.41501	-291.43406	-291.4336476	-291.4021776
[H+SiH_4]	-291.86883	-291.91847	-291.94410	-291.91870	-291.88674	-291.91265	-291.93388	-291.9334574	-291.9019874
SiH_4-H	-291.85880	-291.90964	-291.93413	-291.90804	-291.87777	-291.91223	-291.92431	-291.9238877	-291.8936647
[H_2+SiH_3]	-291.88954	-291.93941	-291.96640	-291.93851	-291.90652	-291.93259	-291.95663	-291.9554661	-291.92396
H-H	-1.158274	-1.166254	-1.173794	-1.17011	-1.16000	-1.16305	-1.17264	-1.1723366	-1.1622996
SiH_3	-290.73127	-290.77315	-290.79260	-290.76840	-290.74651	-290.76954	-290.78399	-290.7831295	-290.7616565

Q^a: QCISD/6-311+G**level. Q^b: QCISD/6-311++G(df,pd)level. Q^c: QCISD/CC-PVTZ level. $MRCI^a$: using CC-PVQZ basis sets. $MRCI^b$: using AUG-CC-PVQZ basis sets.

TABLE-4
REACTION ENTHALPIES ΔH AND POTENTIAL BARRIERS ΔE (Kcal/mol) AT DIFFERENT LEVELS

	Q^a	$G2//Q^a$	$MRCI^a//Q^a$	Q^b	Q^b + ZPE	$G2//Q^b$	$MRCI^b//Q^b$	Q^c	Q^c +ZPE	Exp.
[H+SiH_4]	0.0	0.0	0.0	0.0	0.0	0.0	0.0	0.0	0.0	–
SiH_4-H	+6.42	+5.54	+6.2537	6.68	5.63	4.6573	+6.0052	6.0050	5.1848	–
[H_2+SiH_3]	-12.99	-13.14	-13.99	-12.44	-12.41	-12.78	-14.2731	13.81	13.79	12.39

Q^a : QCISD/6-311+G**level. Q^b: QCISD/6-311++G(df,pd)level. Q^c: QCISD/CC-PVTZ level. $MRCI^a$: using CC-PVQZ basis sets. $MRCI^b$: using AUG-CC-PVQZ basis sets.

TABLE-5
RATE CONSTANTS ($cm^3\ mol^{-1}\ s^{-1}$) FOR THE REACTION $SiH_4 + H \rightarrow SiH_3 + H_2$ IN THE TEMPERATURE RANGE 200-1600 K AT THE G2//QCISD/6-311++G(df,pd) LEVEL

T (K)	TST	CVT	CVT/ZCT	CVT/SCT	ICVT	ICVT/SCT	CVT/SCT[a]	Exp.[b]
200	3.53976E9	1.66754E9	4.20196E9	8.8494E9	1.66754E9	9.8126E9	8.55E11	–
290	7.6454E10	4.35246E10	6.6822E10	9.5116E10	4.35246E10	1.0234E11	6.20E10	1.63E11
300	9.6922E10	5.58054E10	8.3076E10	1.15584E11	5.58054E10	1.24012E11	7.35E10	–
329	1.78192E11	1.05952E11	1.46286E11	1.93242E11	1.05952E11	2.06486E11	1.16E11	3.31E11
330	1.81804E11	1.0836E11	1.49296E11	1.96252E11	1.07758E11	2.10098E11	1.18E11	3.61E11
350	2.6187E11	1.58326E11	2.10098E11	2.69094E11	1.58326E11	2.86552E11	1.57E11	–
379	4.17788E11	2.5886E11	3.2809E11	4.05748E11	2.5886E11	4.29828E11	2.31E11	6.38E11
382	4.37052E11	2.71502E11	3.42538E11	4.22002E11	2.71502E11	4.47286E11	2.40E11	7.04E11
400	5.65278E11	3.5518E11	4.38256E11	5.30362E11	3.5518E11	5.60462E11	2.99E11	–
449	1.04146E12	6.6822E11	7.8862E11	9.1504E11	6.6822E11	9.632E11	5.13E11	1.47E12
496	1.69764E12	1.1137E12	1.2642E12	1.43276E12	1.1137E12	1.505E12	8.07E11	2.4E12
500	1.75784E12	1.15584E12	1.31236E12	1.48092E12	1.15584E12	1.55316E12	8.37E11	–
570	3.1906E12	2.1371E12	2.34178E12	2.57656E12	2.1371E12	2.69094E12	1.48E12	3.67E11
600	3.97922E12	2.68492E12	2.90164E12	3.16652E12	2.68492E12	3.29896E12	1.84E12	4.12E12
658	5.83338E12	3.96718E12	4.22002E12	4.53306E12	3.96718E12	4.71366E12	2.67E12	6.33E12
800	1.2341E13	8.5484E12	8.7892E12	9.2708E12	8.5484E12	9.5718E12	5.65E12	–
1000	2.67288E13	1.8662E13	1.88426E13	1.94446E13	1.8662E13	2.01068E13	1.25E13	–
1200	4.76784E13	3.32906E13	3.33508E13	3.40732E13	3.32906E13	3.50966E13	2.32E13	–
1400	7.525E13	5.25546E13	5.23138E13	5.31566E13	5.25546E13	5.46616E13	3.82E13	–
1600	1.08962E14	7.6454E13	7.5852E13	7.6454E13	7.6454E13	7.8862E13	5.75E13	–

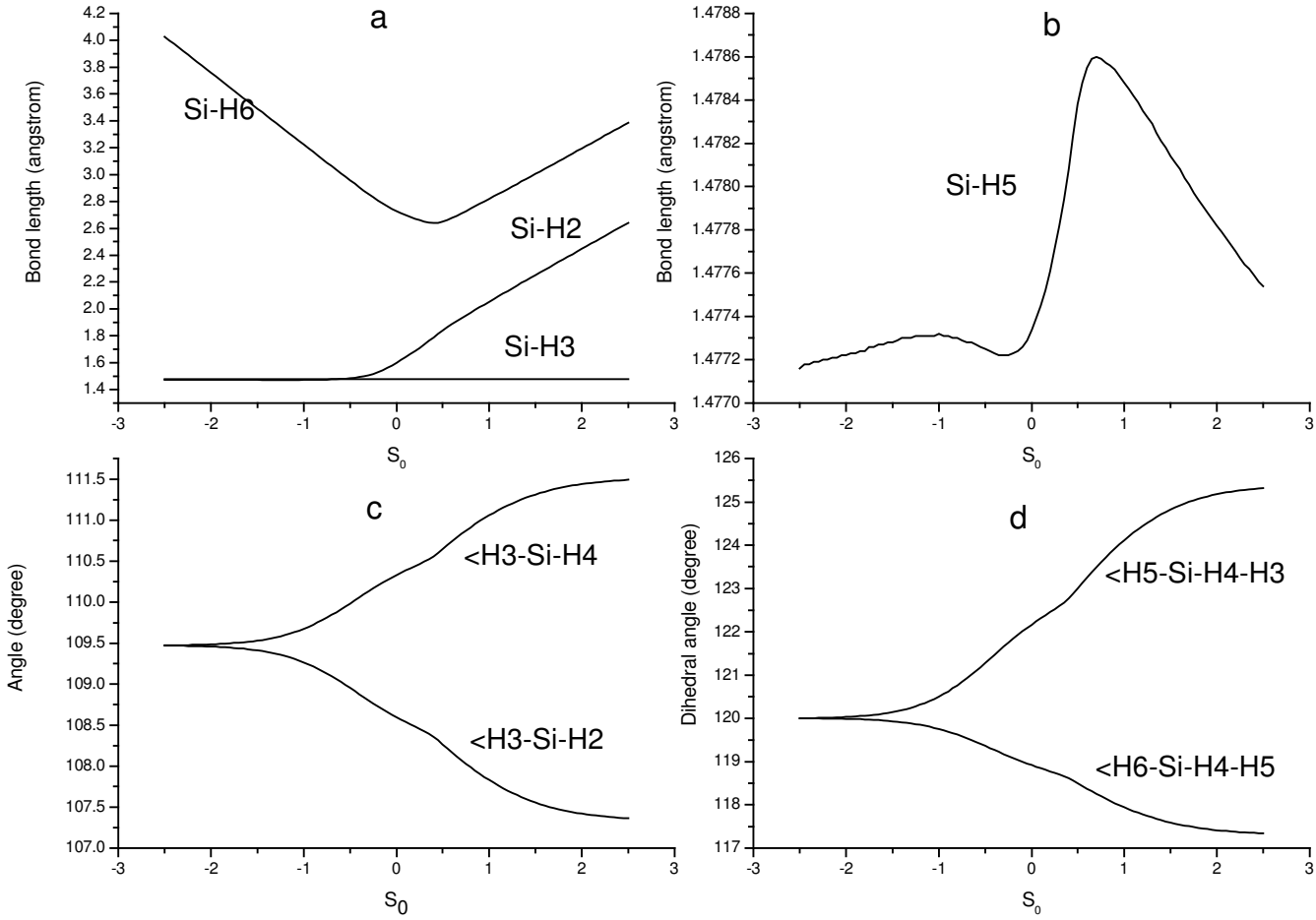

Fig. 2. Main geometry parameters varying with the reaction coordinate at the QCISD/6-311++G(df,pd) level

CC-PVTZ level, the transition state of the exchange reaction has a C_{3V} symmetry which is similar to earlier theoretical calculation. But in the transition state structure, the length of bond Si-H2 which will be broken increase by 6 %, while the length of H2-H6 bond that will be from hydrogen molecule is 60 % larger than the equilibrium bond length of the hydrogen molecule. So the transition state structure of the exchange reaction is reactant-like, furthermore the reaction is exothermic, then the reaction will proceed *via* early transition state according to the Hammond's postulate[23].

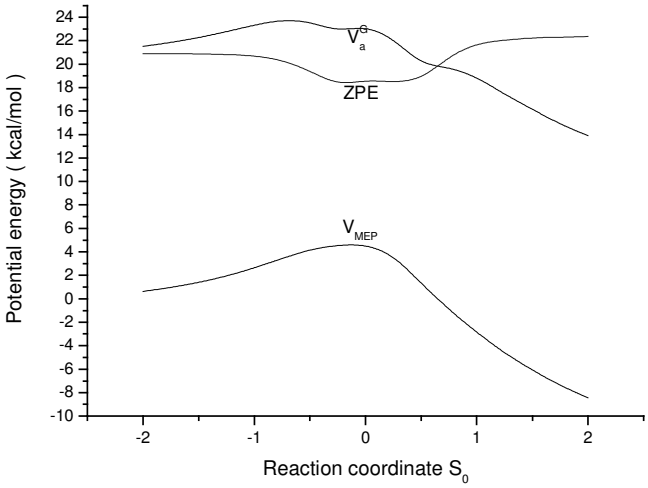

Fig. 3. Classical potential energy, vibrationally adiabatic potential energy and the ZPE curves as functions of s for the reaction $SiH_4 + H \rightarrow SiH_3 + H_2$ at theG2//QCISD level

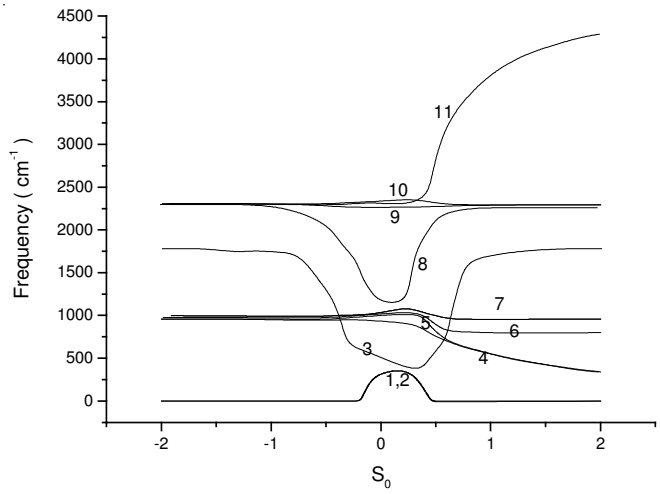

Fig. 4. Changes of the generalized normal-mode vibrational frequencies as functions of s for the reaction $SiH_4 + H \rightarrow SiH_3 + H_2$ at theG2//QCISD level

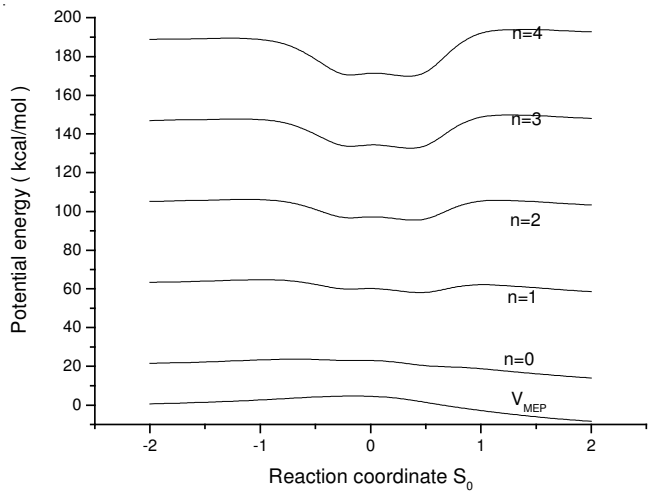

Fig. 5. Potential energy curves of the VMEP plus the vibrational energy ε_n (n = 0, 1, 2, 3, 4) along the reaction path

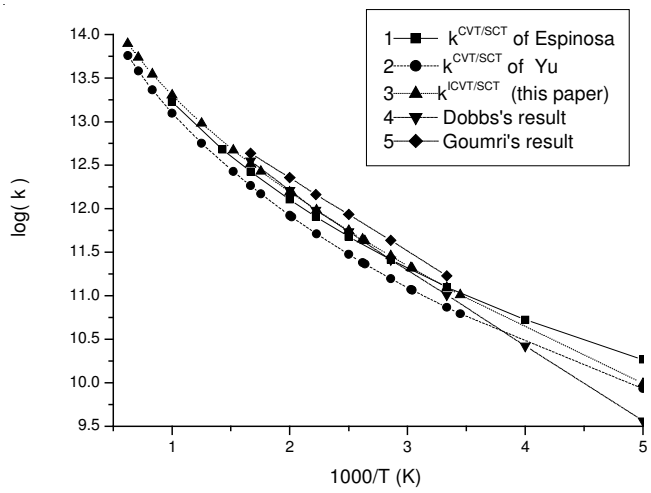

Fig. 6. Forward rate constants including theoretical and experimental results for the reaction $SiH_4 + H \rightarrow SiH_3 + H_2$ at the G2//6-311++G(df,pd) level

Table-2 lists the harmonic vibrational frequencies of the stationary points obtained at the three levels. The frequency analysis reveals that the transition state has one and only one imaginary frequency. The larger imaginary frequency will narrow the potential barrier and over estimate the tunneling correction. Among the reported results, the numbers of the imaginary frequency calculated at the QCISD is lowest than those obtained at the MP2/6-31G* (1880i) and G2 levels (1463i). Furthermore, the value of 1332i calculated at the QCISD/CC-PVTZ is lowest in the three QCISD levels.

Recently, more and more evidences[24] indicate that the van der Walls complexes played an important role in the ground state reaction dynamics even though these complexes occur at considerably larger internuclear distances than those of transition states. Accordingly, many works are performed concerning the issue[25]. In this paper, two van der Walls complexes are found whose formations change the topology properties of the potential energy surface. A high accuracy potential energy surface should reflect the fine structure. Therefore, attention should be paid to them. The role of the van der Walls complexes is expected the verification of the dynamic calculation.

Tables 3 and 4 list the energy of stationary points, reaction enthalpies and potential barriers, respectively. The potential barriers obtained at the G2//QCISD/6-311++G(df,pd) level and G2//QCISD/6-311+G** level take the values 4.66 and 5.54 kcal/mol. Obviously, the former decreases the potential barriers by near 1 kcal/mol than the latter. What's more, the enthalpies are -12.78 and -13.14 kcal/mol, respectively, while the experimental value is -12.39 kcal/mol. Therefore the combination of G2//QCISD/6-311++G(df,pd) is prior to that of G2//QCISD/6-311+G**. On the other hand, the potential barrier and enthalpy is 4.66 and -13.79 kcal/mol, respectively. The potential barrier agrees well with the experimental result but the enthalpy agrees poor.

Properties of the reaction path: For the sake of convenience to describe the reaction process, the atomic numbers are labeled in **Scheme-I**. Starting from the transition state to the reactants or products, the minimum energy paths of the reactions is calculated at the QCISD/6-311++G(df,pd) level by the intrinsic reaction coordinate theory. The profile of

reaction path is drawn in Fig. 1. It can be seen that: firstly, when reactants, *i.e.*, H and SiH_4, approach each other, the complex IM1 is formed directly, then the energy decreases and a flat potential well comes into being. Then the potential energy increase when the atom H continues to approach the SiH_4 molecule and the bond between H2-Si1 breaks up. Subsequently, the transition state is formed. After the system crosses the potential barrier, the H2 atom will apart from SiH_3 with H6 atom, another complex IM2 comes into being. Lastly hydrogen molecule and SiH_3 radical are produced.

The main geometry parameters varying with the reaction coordinate are listed in Fig. 2. Part a reflects the change of bonds, where it can be seen clearly that the H6 atom approaches the Si atom firstly and then departs from Si atom with the H2 atom. During the process, though the change of those bonds between the Si atom and other three H atoms is very small, the change is not monotonic which is drawn intuitionisticly in curve b. Curve c and d show the change of the bond angles and dihedral angles, respectively.

The energy should be emendated on higher level after the key points on the minimum energy path are obtained. A widely acceptable idea is that the geometry is optimized at a low level and the energy is calculated at a high level which can economize the computer time rapidly with the precondition of holding the dependable accuracy. The direct dynamics can be performed after the energies are corrected.

Fig. 3 shows the classical potential energy, vibrationally adiabatic potential energy and the ZPE curves as functions of s. The curve shape is very similar to the previous calculations. The ZPE curve has a shallow well near s = 0 (amu)1/2 bohr. The changes of the generalized normal-mode vibrational frequencies as functions of s are drawn in Fig. 4. It can be seen that vibtational model 1, 2, 6, 7 and 10 have small frequency packages while model 3 and 8 have sharp wells which induces a well on the zero point energy curve. The system has 9, 7 and 11 nonzero frequencies at the reactants, the products and transition state, respectively. The degrees of freedom can be separated into three types: spectator modes, transitional modes and reactive mode[17]. The spectator modes are those that remain basically unchanged in going from reactants to the transition state and they are related to motions which are not directly involved in the reaction. The transitional modes appear along the reaction path as a consequence of transformation of free rotations or free translations at the reactant or product limits into real vibrational motions in the global system. Their frequencies tend asymptotically to zero at the reactant and product limits and reach their maximum in the saddle point zone. The reactive mode is directly involved in the hydrogen transfer and corresponds to a Si-H stretching mode at the reactant, evolving to the H-H stretching mode at the product. This behaviour is similar to that found in other hydrogen abstraction reactions[26-32]. Clearly, mode 4, 6, 7, 9 and 10 belong to spectator modes; mode 1 and 2 belong to transitional modes; mode 3 and 8 belong to reactive modes. Fig. 5 shows the potential energy curves of the V_{MEP} plus the vibrational energy ε_n (n = 0, 1, 2, 3, 4) along the reaction path. The shape of potential curves with n = 0, 1 is similar to that of the MEP, *i.e.*, potential barrier is come into being in the transition state region. While n ≥ 2, potential wells appear near the transition state which implies that the system is easy to be bounded to form the scattering resonance states which are called Feshbach resonace. What's more, a shallow two-potential-well structure is found which reflects the change of the zero point energy. Same phenomenon can be found in height-light-height system, such as I + HI, Br + HBr system.

Rate constant calculation: The CVT and ICVT rate constants with a SCT and ZCT correction for the exchange reaction are calculated in a wide temperature range from 200 k to 1600 K ate the G2//QCISD/6-311+G(df,pd) level. The results of different methods are listed in Table-5. The comparison with other theoretical results and experimental ones is displayed in Fig. 6.

It can be seen that the results of TST are about 2 and 1.5 times of those of CVT and ICVT at low and high temperature, respectively, which implies that the variational effect is small. After tunneling correction, the results of CVT/ZCT and CVT/SCT are 2.5 and 5.3 times of those of TST at low temperature. However the results of CVT/ZCT are lower slightly than those of TST. For the results of ICVT/ZCT and ICVT/SCT, the same change can be found. In the higher temperature range, the ICVT/SCT rate constants are asymptotic to the rate constants of TST and CVT/SCT, which means only in the lower temperature range the SCT correction plays an important role. The newest results are reported in ref.[33-35].

In Fig. 6, line 1 is the results of VTST calculated on semiempirical potential energy surface by Espinosa which is the highest one at low temperature in several theoretical reports and is close to the experimental results at high temperature. Line 2 is the results of VTST calculated at G2//QCISD/6-311+G** level which is agreement with experimental results at low temperature but has a deviation amplitude at high temperature. Line 3 draws the results obtained at the G2//QCISD/6-311++G(df,pd) level which are improved significantly and agree well with the experimental ones in a biggish temperature rang. Line 4 is the results reported by Dobbs which agree well with experimental results at high temperature but has big deviation amplitude at low temperature. Line 5 is the experimental results. Totally, all the theoretical results are lower than the experimental ones. The results reported in this paper, *i.e.*, line 3 and line 4, agree well with the experimental ones in big temperature range.

Conclusion

In this letter, the reaction of H with SiH_4 has been studied using the TST (CVT, ICVT) method with the SCT correction. Rate constants in the temperature range of 200-1600 K were reported at the G2//QCISD/6-311+G(df,pd) level. Several major conclusions can be drawn from this calculation: The structure of reaction paths includes the reactants, the prior complex, the transition state, the post-complex and the product. The reaction is more exothermic and proceeds *via* an earlier transition state. The resonance states are predicted. Along the reaction coordinates, the dynamic potential wells correspond to the Feshbach resonance. The calculated rate constants exhibit typical non-Arrhenius behaviour. The viriational effect on th values of rate constant is small and the tunneling correction is important in the calculation of rate constants in the lower temperature range. The three parameters expression in the

range 200-1600 K is $K = 4.96 \times 10^{7.39} T^{1.92} \exp(-1238.7/T)$ cm^3 mol^{-1}. The calculated ICVT/SCT rate constants are in good agreement with the available experimental data.

ACKNOWLEDGEMENTS

This work is supported by National Natural Science Foundation of China (No.20903062 and 21177076), Natural Science Foundation of Shandong Province (No. Q2008B07), Independent Innovation Foundation of Shandong University (No. 2010TS064 and 2009JC016) and Open Project from State Key Laboratory of Environmental Chemistry and Ecotoxicology, Research Center for Eco-Environmental Sciences, Chinese Academy of Sciences (No. KF2009-10). The authors thank Professor Donald G. Truhlar for providing the POLYRATE 9.7 program.

REFERENCES

1. J.R. Doyle, D.A. Doughty and A. Gallagher, *J. Appl. Phys*., **69**, 4169 (1991).
2. M.J. Kushner, *J. Appl. Phys*., **62**, 2803 (1987).
3. M.J. Kushner, *J. Appl. Phys*., **63**, 2532 (1988).
4. A. Talbot, J. Arcamone, C. Fellous, F. Deleglise and D. Dutartre, *Mater. Sci. Semi-Condut. Proc*., **8**, 21 (2004).
5. P. Duan, Z.X. Wang, Y. Liu, J.Y. Liu and X.G. Wang, *Chem. Phys. Lett*., **22**, 405 (2005).
6. N.L. Arthur, P. Porzinger, B. Reimann, H.P. Steenbergen, *J. Chem. Soc. Faraday Trans*., **2**, **85**, 1447 (1989).
7. A. Goumri, W.J. Yuan, L.Y. Ding, Y.C. Shi and P. Marshall, *Chem. Phys*., **177**, 33 (1993).
8. H. Niki and G.J. Mains, *J. Phys. Chem*., **68**, 304 (1964).
9. J.A. Cowfer, K.P. Lynch and J.V. Michael, *J. Phys. Chem*., **79**, 1139 (1975).
10. K.Y. Choo, P.P. Gaspar and A.P. Wolf, *J. Phys. Chem*., **79**, 1752 (1975).
11. E.A. Austin and F.W. Lampe, *J. Phys. Chem*., **81**, 1134 (1977).
12. M. Koshi, F. Tamura and H. Matsui, *Chem. Phys. Lett*., **173**, 235 (1990).
13. D. Mihelcic, V. Schubert, R.N. Schindler and P. Potzinger, *J. Phys. Chem*., **81**, 1543 (1977).
14. M.S. Gordon, D.R. Gano and J.A. Boatz, *J. Am. Chem. Soc*., **105**, 5771 (1983).
15. A. Tachibana, Y. Kurosaki, K. Yamaguchi and T. Yamabe, *J. Phys. Chem*., **95**, 6849 (1991).
16. K.D. Dobbs and D.A. Dixon, *J. Phys. Chem*., **98**, 5290 (1994).
17. J. Espinosa-Garcia, J. Sanson and J.C. Corchado, *J. Chem. Phys*., **109**, 466 (1998).
18. X. Yu, S.M. Li, Z.S. Li and C.C. Sun, *J. Phys. Chem. A*, **104**, 9207 (2000).
19. M.H. Wang, X.M. Sun, W.S. Bian and Z.T. Cai, *J. Chem. Phys*., **124**, 234311 (2006).
20. L.A. Curtiss, K. Raghavachari, G.W. Trucks and J.A. Pople, *J. Chem. Phys*., **94**, 7221 (1991).
21. M.J. Frisch, G.W. Trucks and J.A. Pople, Gaussian, Inc., Pittsburgh PA (2003).
22. J.C. Corchado, Y.Y. Chuang, P.L. Fast, J. Villa, W.P. Hu, Y.P. Liu, G.C. Lynch, K.A. Nguyen, C.F. Jackels, V.S. Melissas, B.J. Lynch, I. Rossi, E.L. Coitino, A.F. Ramos, J. Pu, T.V. Albu, R. Steckler, B.C. Garrett and D.G. Truhlar, POLYRATE version 9.3 (2003).
23. G.S. Hammond, *J. Am. Chem. Soc*., **77**, 334 (1955).
24. D.M. Neumark, *Phys. Chem. Commun*., **5**, 76 (2002).
25. R.L. Wilson, Z.M. Loh, D.A. Wild, E.J. Bieske and A.A. Buchachenko, *J. Chem. Phys*., **121**, 2085 (2004).
26. J.C. Corchado and J. Espinosa-Garcia, *J. Chem. Phys*., **105**, 3160 (1996).
27. J. Espinosa-Garcia and J.C. Corchado, *J. Chem. Phys*., **105**, 3517 (1996).
28. J. Espinosa-Garcia and J.C. Corchado, *J. Phys. Chem*., **100**, 16561 (1996).
29. J.C. Corchado and J. Espinosa-Garcia, *J. Chem. Phys*., **106**, 4013 (1997).
30. J. Espinosa-Garcia and J.C. Corchado, *J. Phys. Chem. A*, **101**, 7336 (1997).
31. J. Espinosa-Garcia and J.C. Corchado, *J. Chem. Phys*., **101**, 1333 (1994).
32. J. Espinosa-Garcia and J.C. Corchado, *J. Chem. Phys*., **101**, 8700 (1994).
33. M.H. Wang, X.M. Sun and W.S. Bian, *J. Chem. Phys*., **129**, 084309 (2008).
34. M.H. Wang, X.M. Sun, W.S. Bian and Z.T. Cai, *J. Chem. Phys*., **124**, 234311 (2006).
35. J.W. Cao, Z.J. Zhang, C.F. Zhang, K. Liu, M.H. Wang and W.S. Bian, *Proc. Nat. Acad. Sci. USA*, **106**, 13180 (2009).